Draft version February 1, 2008
Preprint typeset using LaTeX style emulateapj v. 04/21/05

SUBARU HDS OBSERVATIONS OF A BALMER-DOMINATED SHOCK IN TYCHO'S SUPERNOVA REMNANT *

Jae-Joon Lee,[1,2] Bon-Chul Koo,[1] John Raymond,[3] Parviz Ghavamian,[4] Tae-Soo Pyo,[5] Akito Tajitsu,[5] and Masahiko Hayashi[5]

Draft version February 1, 2008

ABSTRACT

We present an Hα spectral observation of a Balmer-dominated shock on the eastern side of Tycho's supernova remnant using SUBARU Telescope. Utilizing the High Dispersion Spectrograph (HDS), we measure the spatial variation of the line profile between preshock and postshock gas. Our observation clearly shows a broadening and centroid shift of the narrow-component postshock Hα line relative to the Hα emission from the preshock gas. The observation supports the existence of a thin precursor where gas is heated and accelerated ahead of the shock. Furthermore, the spatial profile of the emission ahead of the Balmer filament shows a gradual gradient in the Hα intensity and line width ahead of the shock. We propose that this region ($\sim 10^{16}$ cm) is likely to be the spatially resolved precursor. The line width increases from ~ 30 km s^{-1} up to ~ 45 km s^{-1} and its central velocity shows a redshift of ~ 5 km s^{-1} across the shock front. The characteristics of the precursor are consistent with a cosmic ray precursor, although a possibility of a fast neutral precursor is not ruled out.

Subject headings: ISM:supernova remnants – ISM: individual (Tycho, G120.1+1.4) – Shock Waves – line: profiles

1. INTRODUCTION

Balmer-dominated filaments are the signature of non-radiative shocks propagating into partially neutral medium (Chevalier & Raymond 1978). The Hα line profile is composed of two distinctive components (narrow and broad) representing the velocity distribution of preshock and postshock gases, respectively (Chevalier et al. 1980). High resolution spectroscopic observations of several of these shocks have revealed that the width of the narrow component is unusually large ($30 \sim 50$ km s^{-1}) for ambient neutral hydrogen, and it was proposed that the gas was heated in a precursor thin enough ($\lesssim 10^{17}$ cm) to avoid complete ionization of hydrogen (see Ghavamian et al. 2001; Sollerman et al. 2003, and references therein).[6] Two likely candidates are cosmic-ray (CR) and fast neutral precursors (Smith et al. 1994; Hester et al. 1994; Ghavamian et al. 2001). Both scenarios predict significant Doppler shifts of preshock gas. No clear indication of such a shift of the Hα narrow component is reported (but see Lee et al. 2004). A careful comparison of postshock and preshock line profiles with high spectral resolution is crucial for confirming the existence of such a precursor.

The blast wave of Tycho's SNR, the historical remnant of the 1572 supernova, has been known to exhibit Balmer-dominated emission (van den Bergh 1971; Kamper & van den Bergh 1978). The region of the brightest Hα emission (Knot g from Kamper & van den Bergh 1978) is located along the north-eastern edge of the remnant. Faint, diffuse optical emission extends $\sim$1 pc ahead of the Balmer-dominated filaments (Ghavamian et al. 2000, G00 hereafter). This feature has been identified as a photoionization precursor (PIP) produced by photoionization of the preshock gas by He II λ304Å emission from behind the blast wave (G00). The estimated temperature of the PIP is $\sim 1.2 \times 10^4$ K, which is not high enough to explain the observed width of the Balmer narrow component.

The existence of Hα emission from the PIP makes Tycho an unique target for the study of nature of the thin precursor, as we can investigate the change of the line profile across this precursor by comparing the line emission from the PIP (preshock) and that of Knot g (postshock). In this *Letter*, we present high resolution (Echelle) long slit Hα spectra of Tycho Knot g and its PIP using the SUBARU High Dispersion Spectrograph (Noguchi et al. 2002). Our observations reveal the line broadening and the Doppler shift of the the narrow component, providing strong evidence for the existence of a cosmic ray or fast neutral precursor.

2. OBSERVATIONS AND RESULTS

The spectrosopic observation was carried out on 2004 October 1. Longslit Echelle spectroscopy of the Hα line was performed using order-blocking filters (HDS standard setup "stdHa"). This gives a spectral coverage of 6540 Å$\sim$ 6690 Å over the 60″ of slit length. The slit was centered at $\alpha(2000)$, $\delta(2000)$ = ($00^{\rm h}$ $25^{\rm m}$ $56\overset{\rm s}{.}5$, 64° $09'$ $28''$) with position-angle of 76° (measured E of N), covering both Knot g and its PIP simultaneously (Fig. 1(a)). A total of 3×30 minutes of source exposure was obtained, and the same amount of exposure for

*BASED ON DATA COLLECTED AT SUBARU TELESCOPE, WHICH IS OPERATED BY THE NATIONAL ASTRONOMICAL OBSERVATORY OF JAPAN

[1] Astronomy Program, Department of Physics and Astronomy, Seoul National University, Seoul 151-742, Korea
[2] jjlee@astro.snu.ac.kr
[3] Harvard-Smithsonian Center for Astrophysics, 60 Garden Street, Cambridge, MA 02138
[4] Department of Physics and Astronomy, Johns Hopkins University, 3400 North Charles Street, Baltimore, MD 21218
[5] Subaru Telescope, National Astronomical Observatory of Japan, 650 North A'ohōkū Place, Hilo, HI 96720

[6] We refer to this precursor explicitly as a "thin precursor", to avoid potential confusion with a photoionization precursor which will be shortly introduced.

nearby sky. The spectrum was binned by 2 along the slit direction and 4 along the dispersion direction before the readout. The pixel scale after the binning is $0.27''$ pixel^{-1} (9.3×10^{15} cm pixel^{-1} at a distance of 2.3 kpc (Kamper & van den Bergh 1978)) and 0.08 Å respectively. The slit width was $2''$, which gives velocity resolution of 17 km s^{-1}. The seeing was $0\farcs5 \pm 0\farcs1$. The processing of the SUBARU data included a typical CCD preprocessing (including overscan correction and flat fielding) and two-dimensional spectral extraction. A wavelength calibration solution is obtained from the spectrum of a Th-Ar lamp. The source spectrum was sky-subtracted, and normalized using the spectra of standard stars. The uncertainty in the wavelength calibration is estimated to be around 0.2 km s^{-1} at the wavelength of Hα.

In Fig. 1(b), we present the fully processed two dimensional spectrum of Hα line. The bright patch at the bottom with three distinct local emission peaks corresponds to Knot g, and the faint emission extending to the top of the image corresponds to the PIP. The average Hα spectrum of Knot g and that of PIP are shown together in Fig. 2. The velocity width of the Knot g narrow component line is clearly larger than that of the PIP Hα line. In addition, the velocity centroid of the Knot g narrow component is slightly redshifted (5.5 ± 0.6 km s^{-1}) relative to that of the PIP Hα line. And as clearly seen in Fig. 2(b), the Knot g spectrum shows a very broad ($\sim$ 1,000 km s^{-1}), faint Hα line. The small peak near 900 km s^{-1} is the [N II] λ6583.4 Å line from the PIP.

The spectrum of the PIP is well fitted by a single Gaussian, and yields a FWHM of 33.8 ± 0.8 km s^{-1} and centroid velocity of -35.8 ± 0.6 km s^{-1} (in LSR frame).[7] The measured FWHM of [N II] λ6583.4 Å in the PIP is ~ 23 km s^{-1}. If the broadening were purely thermal, the widths of the lines whould be inversely proportional to the square root of their atomic masses. The expected width of the [N II] line in this case is $1/\sqrt{14} = 0.267$ of Hα. As this is significantly narrower than what is observed, a significant amount of nonthermal broadening is suggested. If we simply assume that the observed line widths are a convolution of thermal and nonthermal broadenings, the estimated thermal temperature is $\sim 13,000$ K, consistent with 12,000 K of G00. It is also possible that the large line width is due to a residual of Galactic Hα emission.

An adequate fit to the Knot g spectrum requires three Gaussian components. They have velocity widths of 45.3 ± 0.9 km s^{-1} (narrow), 108 ± 4 km s^{-1} (intermediate) and 931 ± 55 km s^{-1} (broad), with central velocities of -30.3 ± 0.2, -25.8 ± 0.8 and 29 ± 18 km s^{-1}, respectively. This result confirms that the Hα narrow component line of Knot g is redshifted and broadened relative to that of the PIP. The broad component (FWHM$\sim$ 1,000 km s^{-1}) should correspond to the previously reported $\sim$ 2,000 km s^{-1} component (Ghavamian et al. 2001). The relatively narrower width of our observation is probably due to the insensitivity of our spectroscopic configuration to the very broad line, although the possibility of temporal variation (e.g., by crossing a density jump) does exist. The abrupt density increase might be possible if the shock is propagating into the edge outskirts of the dense cloud (Lee et al. 2004). The existence of the intermediate width component has already been reported by G00. It may be produced when slow protons picked up by the postshock magnetic field undergo a secondary charge exchange. Alternatively, it might be an artifact of the assumption of Gaussian distributions, which would not necessarily be appropriate if the motions are non-thermal.

The characteristics of the narrow component Hα line of Knot g are consistent with G00, except that the velocity centroid of the line in our data is significantly different from theirs ($v_{\rm LSR} = -30.3 \pm 0.2$ from our data vs. -53.9 ± 1.3 km s^{-1} from G00). We have carefully assessed our wavelength calibration, but couldn't find any significant source of error. The wavelengths of night sky lines observed near Hα matched well with those of VLT UVES night-sky emission line catalog (Hanuschik 2003) within error of 0.02 Å (~ 1 km s^{-1}). The Hα spectrum of blank sky is also consistent with nearby WHAM spectra (Haffner et al. 2003). Furthermore, the central velocity of [N II] λ6583.4 Å emission line from the PIP is consistent with that of Hα. Although we believe that our wavelength calibration solution is quite secure, the discrepancy with the previous observation should be confirmed by an independent observation. For the rest of this paper, we mainly concentrate on the line width and the relative variation of central velocity.

3. LOCATION OF THE SHOCK FRONT AND DISCOVERY OF A THIN (10^{16} CM) PRECURSOR

Fig. 3 shows the spatial variation of the Hα line profile along the slit. In the top panel, we separately plot the integrated intensities of the representative Hα of narrow and broad components, together with their sum (refer to the figure caption for the velocity range of each component). In the middle and bottom panels, we plot the central velocities and FWHMs at each slit position from the *single* Gaussian fit to the full profile. In all three panels, the x-axis represents the pixel offset from the southwest end of the slit. Although three Gaussian components are actually required to adequately fit the Hα profile of Knot g, the non-uniqueness of the multiple-component fitting can complicate the interpretation of the different emission line components. Therefore, we plot the fit result from a single Gaussian and describe our interpretation of this fit in the region of Knot g as following: First, the central velocities closely match those of the narrow component. Fitting with multiple components leaves the fitted line centroids unchanged to within the errors. Second, the FWHMs basically trace the spatial variation of the narrow component width, but the presence of the intermediate and the broad components contribute significantly to the width. When fit with three Gaussian components, the large widths of the Hα narrow component in Knot g from the single profile models ($60 \sim 80$ km s^{-1}) are reduced to $40 \sim 50$ km s^{-1}.

Inspection of Fig. 3 reveals that there exists only one location (pixel offset 27, marked as a dotted vertical line) where the intensity and width of the Hα line exhibits an abrupt jump. The jump is most noticeable for the broad component, where the flux is virtually zero toward the direction of ambient medium (i.e., toward positive pixel off-

[7] throughout this paper, we give line widths corrected for instrumental broadening and velocity in LSR frame.

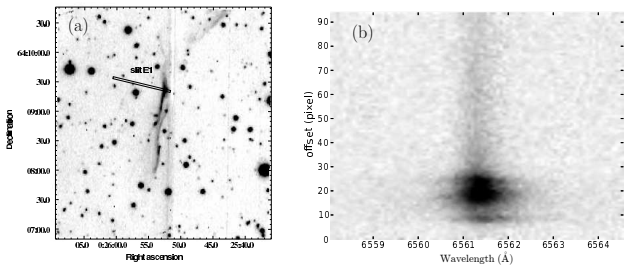

FIG. 1.— (a) Hα image of Tycho Knot g with position of the $2'' \times 60''$ slit overlaid. (b) The fully-processed Hα 2-d spectrum (only the western part of the slit is shown). The bright emission knot at the bottom is Knot g.

sets). The central velocity of the narrow component also shows rapid change around this location. The FWHM also steeply increases behind this point, but this might be largely due to the sudden appearance of the broad component. The fact that the intensity of the broad component, which is associated with the postshock gas, shows a significant jump at this location suggests that it corresponds to the location of the shock front.

The Hα intensity in the PIP region is nearly constant along the slit, but shows an rapid rise just before the shock front, i.e., from pixel offset 32 to 27 in Fig. 3. The intensity of the Hα line in the PIP region is about 10% of the observed peak value in Knot g, and it reaches about half the peak very near the shock. The line width also increases from 30 to 45 $\mathrm{km\,s^{-1}}$ within this region. We propose that the steep increase of the Hα intensity accompanied with line broadening corresponds to a thin precursor where gas is heated and accelerated. Unlike the line broadening, the observed velocity centroids shift slightly behind the shock instead of the precursor region. This does not necessarily indicate that the broadening and the Doppler shift takes at different region as this is likely due to geometrical projection effects. The Hα intensity profile gives an e-folding thickness of 1.4 ± 0.4 pixel (after accounting for seeing), which corresponds to $(1.4 \pm 0.4) \times 10^{16}$ cm at a distance of 2.3 kpc.

The observed emission of Knot g shows a few local peaks indicating possible substructure, e.g., a collection of shock tangencies seen in projection along the line of sight. This leads to a possibility that the 'precursor' is simply the results of geometric projection of fainter Balmer-dominated filament lying just ahead of Knot g. If we assume that this filament has a line profile similar to that of Knot g, i.e., have a same broad-to-narrow ratio, then a detectable amount of broad component is expected. The flux profile of broad component plotted in Fig. 3 would show similar gradual increase in the precursor region, which is not seen. Also, no hint of a broad component is found in a summed spectra of precursor region, which is expected to show up. Examining the archival *Chandra* observation of Tycho's SNR (the analysis is presented by Warren et al. 2005), we did not find evidence of X-ray emission extending ahead of Knot g. Therefore, there is no strong supporting evidence in favor of a projection, although we cannot rule out the possibility.

4. NATURE OF THE THIN PRECURSOR

As the shock is nearly tangential to our line of sight, the actual amount of bulk gas acceleration could be much

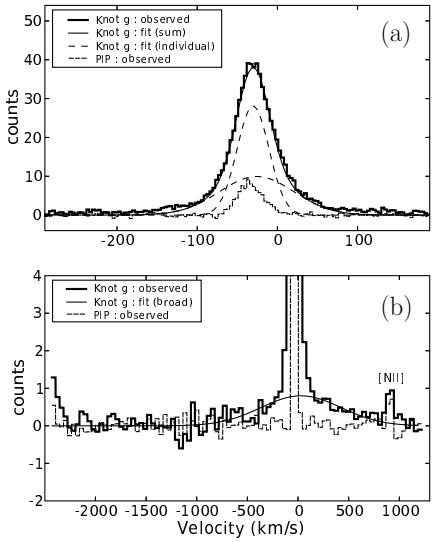

FIG. 2.— (a) Hα spectrum of Knot g and the PIP. The spectrum of Knot g is fitted with three Gaussian components, and two narrowest components are displayed (thin dashed) together with their sum (thin solid). (b) Same as (a) except the full observed velocity range is presented and the spectra are binned. The Knot g broad component from the above fit is displayed as a thin solid line.

larger than the observed Doppler shift. The shock angle can be inferred from the radial velocity shift of the broad component of Knot g relative to the narrow component (Chevalier et al. 1980), which is measured to be $\sim 60\ \mathrm{km\,s^{-1}}$. As our observation could be insensitive to this broad component, using this value is rather conservative. On the other hand, Ghavamian et al. (2001) reported a redshift of $\sim 130\ \mathrm{km\,s^{-1}}$, but their field of view is different from ours. We take these two values as limits and give shock angle of $2^\circ - 5^\circ$ assuming a shock velocity of 2,000 $\mathrm{km\,s^{-1}}$. We consider 5 $\mathrm{km\,s^{-1}}$ to be the representative redshift of the narrow component compared to unperturbed medium, which gives actual acceleration of $60 \sim 130\ \mathrm{km\,s^{-1}}$.

The line width of the narrow component at the shock front ($\sim 45\,\mathrm{km\,s^{-1}}$) corresponds to a neutral hydrogen temperature of 40,000 K, if the line broadening is purely thermal, or lower, if there is a significant non-thermal broadening such as a wave motion. Neutral hydrogen atoms and protons may have similar velocity distributions due to their charge exchange interactions. But that of electrons can be different, which would depend on the heating mechanism in the precursor. In the following, we estimate the electron temperature in the thin precursor (TP) from the observed intensity increase of factor 5. Since the observed spectrum is an integrated emission along the line of sight where a significant contribution from PIP region is expected, the actual emissivity increase within the precursor should be much greater. We assume that regions of the PIP and the TP are represented by two concentric shells with thicknesses of $\delta_{\mathrm{PIP}} \simeq 10^{16}\,\mathrm{cm}$ and $\delta_{\mathrm{TP}} \simeq 1\,\mathrm{pc}$ (G00), respectively, and that both have an inner diameter of the Tycho (5.4 pc). Then the ratio of path length through each shell along the tangential direction of the shock front is $\simeq 18$. This implies that the emissivity increase in the TP could be as large as a factor of 90. This value should be regarded

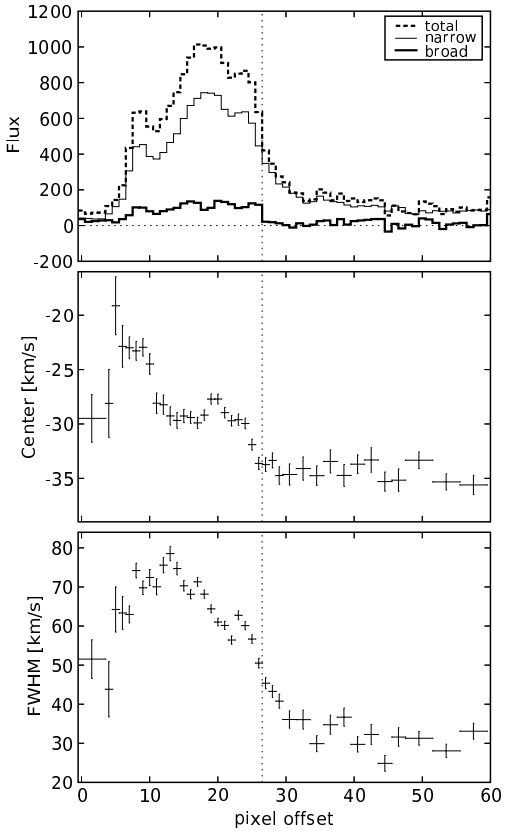

FIG. 3.— (top) Integrated fluxes along the slit position of Hα spectrum for a given velocity range. The thin solid line shows emission in the range $-60 < v_{\rm LSR} < 10$ km s^{-1}, representative of Hα narrow component, while the thick solid line shows emission in the range $-400 < v_{\rm LSR} < -120$ km s^{-1} and $+100 < v_{\rm LSR} < +350$ km s^{-1}, for the broad component. The thick dashed line shows the summed intensity for both components. ($-400 < v_{\rm LSR} < +350$ km s^{-1}). Middle and bottom panels: central velocities and FWHMs from fits with a single Gaussian. The proposed location of shock front is marked as a vertical dotted line.

as an upper limit as it is likely that the filament is nearly flat and tangent to the line of sight. The collisional excitation rate of Hα at $T_e \sim 40,000$ K is 2,000 times greater than that of 12,000 K which is the temperature of the PIP region (G00). This value greatly exceeds the emissivity increase of 90, and implies a few possibilities. The electron temperature can be less than 40,000 K, either if observed Hα line width has significant nonthermal broadening, or if T_e is intrinsically less than T_p. On the other hand, the estimated emissivity increase might be explained if the emissivity increase due to high T_e is suppressed by ionization of neutrals. Since the existence of Blamer-dominated filaments requires a significant fraction of neutral hydrogen atoms to survive within precursor, this possibility is less favored.

The two likely candidates for this precursor are fast neutral and CR precursors. The momentum and energy carried by upstreaming fast neutrals can be large enough to explain the observed heating and acceleration in the precursor, but the available model calculations do not predict significant heating by these neutrals (Lim & Raga 1996; Korreck 2005). Furthermore, It is difficult to reproduce the small range of FWHMs observed for narrow component Hα lines from shocks of different velocities (Smith et al. 1994; Hester et al. 1994). The observed characteristics of the precursor are consistent with a CR precursor. CR acceleration in the shock does require a precursor (e.g., Blandford & Eichler 1987) and there has been growing evidence of CR acceleration in young SNRs including Tycho itself (e.g., Warren et al. 2005). Significant heating and acceleration are expected to happen in the CR precursor (Blandford & Eichler 1987). Interaction of CR particles in the upstream generates Alfv́en waves and significant amplification of magnetic field has been suggested (Bell & Lucek 2001). Although a measurement of the preshock magnetic field is hardly available, a high value ($40\,\mu$G) of preshock magnetic field is suggested for Tycho (Völk et al. 2002), which may explain the line width of the narrow component.

To conclude, our SUBARU observation clearly has shown the line broadening and the Doppler shift between the preshock gas and postshock gas. This strongly suggests the existence of the thin precursor. Furthermore, the precursor itself is likely to be resolved. Given the lack of observational constraints on CR ion acceleration in SNR shocks, the tentatively measured width ($\sim 10^{16}$ cm) of the thin precursor whose primary candidate is the CR precursor is promising. Follow-up observation, such as a high resolution imaging with *HST*, would clearly resolve the structures of the precursor.

We thank to the anonymous referee for valuable comments. This work was supported by the Korea Research Foundation (grant No. R14-2002-058-01003-0). JJL has been supported in part by the BK 21 program.

REFERENCES

Bell, A. R. & Lucek, S. G. 2001, MNRAS, 321, 433
Blandford, R. & Eichler, D. 1987, Phys. Rep., 154, 1
Chevalier, R. A., Kirshner, R. P., & Raymond, J. C. 1980, ApJ, 235, 186
Chevalier, R. A. & Raymond, J. C. 1978, ApJ, 225, L27
Ghavamian, P., Raymond, J., Hartigan, P., & Blair, W. P. 2000, ApJ, 535, 266
Ghavamian, P., Raymond, J., Smith, R. C., & Hartigan, P. 2001, ApJ, 547, 995
Haffner, L. M., Reynolds, R. J., Tufte, S. L., Madsen, G. J., Jaehnig, K. P., & Percival, J. W. 2003, ApJS, 149, 405
Hanuschik, R. W. 2003, A&A, 407, 1157
Hester, J. J., Raymond, J. C., & Blair, W. P. 1994, ApJ, 420, 721
Kamper, K. W. & van den Bergh, S. 1978, ApJ, 224, 851
Korreck, K. 2005, Ph.D. Thesis
Lee, J., Koo, B., & Tatematsu, K. 2004, ApJ, 605, L113
Lim, A. J. & Raga, A. C. 1996, MNRAS, 280, 103
Noguchi, K., Aoki, W., Kawanomoto, S., Ando, H., Honda, S., Izumiura, H., Kambe, E., Okita, K., Sadakane, K., Sato, B., Tajitsu, A., Takada-Hidai, T., Tanaka, W., Watanabe, E., & Yoshida, M. 2002, PASJ, 54, 855
Smith, R. C., Raymond, J. C., & Laming, J. M. 1994, ApJ, 420, 286
Sollerman, J., Ghavamian, P., Lundqvist, P., & Smith, R. C. 2003, A&A, 407, 249
Völk, H. J., Berezhko, E. G., Ksenofontov, L. T., & Rowell, G. P. 2002, A&A, 396, 649
van den Bergh, S. 1971, ApJ, 168, 37
Warren, J. S., Hughes, J. P., Badenes, C., Ghavamian, P., McKee, C. F., Moffett, D., Plucinsky, P. P., Rakowski, C., Reynoso, E., & Slane, P. 2005, ApJ, 634, 376